Phase transitions of the 6-clock model in two dimensions

1991 J. Phys. A: Math. Gen. 24 265

(http://iopscience.iop.org/0305-4470/24/1/033)

J. Phys. A: Math. Gen. 24 (1991) 265–275. Printed in the UK

Phase transitions of the 6-clock model in two dimensions

Atsushi Yamagata and Ikuo Ono

Department of Physics, Faculty of Science, Tokyo Institute of Technology, Oh-okayama, Meguro-ku, Tokyo 152, Japan

Received 20 July 1990

Abstract. It is confirmed that there exists a Kosterlitz–Thouless (KT) like phase in the ferromagnetic 6-clock model on the square lattice through studies of the interfacial free energy estimated by Monte Carlo simulations. We find that lower and upper transition temperatures are $T_1 = 0.75$ and $T_2 = 0.90$ respectively, and that the critical exponent η for the correlation function in the KT-like phase varies from 0.15 at T_1 to 0.26 at T_2. The correlation length ξ just above T_2 is estimated directly from the magnetization profile, and it is shown to behave as $\xi \sim \exp(bt^{-1/2})$, $t = (T - T_2)/T_2$, as approaching the KT-like phase.

1. Introduction

The 6-clock model has Z_6 symmetry. Each spin can have one of six different directions in the plane of spin space. Its Hamiltonian is described by

$$H = -\sum_{\langle i,j \rangle} \cos(\theta_i - \theta_j) \qquad \theta_i = 2\pi n_i/6 \quad n_i = 0,\ 1, \cdots, 5 \tag{1}$$

where the sum is over nearest-neighbour pairs on the square lattice (In this paper physical quantities are presented in units of the strength J of interactions with $k_B = 1$.)

As is well known, the XY model in two dimensions has no long-range order at any finite temperature (Mermin and Wagner 1966) but a phase transition occurs at a finite temperature T_C (Kosterlitz and Thouless 1973, Kosterlitz 1974). Below T_C its correlation function exhibits a power-law decay with a temperature-dependent exponent η, $\langle \cos(\theta_0 - \theta_r) \rangle \sim r^{-\eta}$. This phase is called the Kosterlitz–Thouless (KT) phase.

José *et al* (1977) first investigated the XY model with p-fold symmetry-breaking fields h_p. In the limit $h_p \to +\infty$ it turns out to be the p-state clock model. This field may be attributed to crystalline field in real magnets and the possible values of p are 2, 3, 4 and 6 due to symmetries of lattices. It was shown by use of the Migdal–Kadanoff real-space renormalization group approximation that the p-state clock model has two phase transitions at T_1 and T_2 ($T_1 < T_2$) when $p > 4$, and that its intermediate phase is the KT phase. Elitzur *et al* (1979) studied a discrete Villain model whose symmetry was Z_p. They showed by using self-duality and correlation inequalities that there exists a disordered and massless phase (the correlation length diverges) if a Villain model (Villain 1975) or a neutral Coulomb gas model (Kosterlitz and Thouless 1973, Chui and Weeks 1976) has a corresponding phase.

0305-4470/91/010265+11$03.50

Tobochnik (1982) simulated the p-state clock model for $p = 4$, 5 and 6 using the Monte Carlo renormalization group (MCRG) method. He found, for $q = 5$ and 6, the intermediate phase in which the critical exponent η for the correlation function varies with temperature. He determined lower and upper transition temperatures to be $T_1 = 0.6$ and $T_2 = 1.3$ respectively and the critical exponent $\eta = 0.10$ at T_1 for $p = 6$. Challa and Landau (1986) carried very large simulations of the 6-clock model and used a finite-size scaling and a fourth-cumulant (FC) method. They obtained $T_1 = 0.68 \pm 0.02$ and $T_2 = 0.92 \pm 0.01$, η varied between 0.100 at T_1 and 0.275 at T_2, and two phase transitions were assigned to be the KT-type.

The phase transitions of the 6-clock model are very interesting in connection with those of the three-state antiferromagnetic Potts (AFP) model (Wu 1982, 1984). It was indicated in two dimensions that the AFP model, modified with weak next-nearest-neighbour ferromagnetic interactions, exhibited a KT-like phase (Ono 1984, Ono and Yamagata 1990), but that the pure AFP model contained a phase transition only at zero temperature (Cardy 1981, Grest and Banavar 1981, Baxter 1982, Jayaprakash and Tobochnik 1982, Wang *et al* 1989).

The purpose of this paper is to confirm the existence of the KT-like phase, and to investigate the phase transition between the intermediate phase and the disordered phase in the 6-clock model in terms of the interfacial free energy through Monte Carlo simulations. In section 2 our method is described. We give the results of simulations in section 3. A summary is given in section 4.

2. Methods

2.1. Monte Carlo simulations

The Metropolis Monte Carlo technique (Metropolis *et al* 1953, Binder 1979, 1984) is used to simulate the behaviour of the model on $N_{\parallel} \times N_{\perp}$ square lattices ($N_{\parallel} > N_{\perp}$, see subsection 2.2). Our analysis is based on the interfacial free energy formed between the coexisting bulk ordered phases (Ueno *et al* 1989). For each lattice we set two types of boundary condition, one of which brings out no interface while the other does: all $N_{\parallel}$ spins on the top and bottom edges of the lattice are fixed to be parallel or anti-parallel for each system, and periodic boundary conditions are imposed on the side edges. To fix spins on the boundaries is equivalent to imposing infinite magnetic fields on these spins. Hereafter we call the above two types of boundary condition the parallel and the anti-parallel boundary condition respectively. The spin-site to be updated is chosen sequentially and an update state is randomly selected among the five states except the current state. The pseudorandom numbers $\{R_n\}$ are generated by the Tausworthe method as follows. The nth random number R_n is given by $R_n = R_{n-250} \oplus R_{n-103}$, where $\oplus$ denotes the 'exclusive-or' operation between binary digits (Ito and Kanada 1988). We start each simulation from a high temperature with a random configuration and then gradually cool the system from it. Energies at a certain temperature are calculated from the averages over 5×10^4 Monte Carlo steps per spin (MCS) after discarding 1×10^4 MCS to attain equilibrium.

2.2. Interfacial free energy

The excess free energy ΔF for a certain temperature is evaluated by numerical integrations of the excess energy ΔE between systems with and without interfaces,

starting from a certain temperature T_0 above the transition temperature. Here we have selected T_0 so that ΔE will be within its standard deviation for the Monte Carlo averages. Thus we have (Ueno *et al* 1989, Ono and Yamagata 1990)

$$\Delta F(T) = \Delta E(T) - T \int_{T_0}^{T} \frac{\mathrm{d}(\Delta E(T'))}{T'}. \tag{2}$$

The interfacial free energy σ is given by $\sigma = \Delta F/N_{\|}$. The finite-size scaling law for the interfacial free energy is assumed to be

$$\sigma(T, N_\perp) \sim N_\perp^{1-d}\, \tilde{\sigma}(N_\perp |t|^{\nu}) \qquad t = (T - T_C)/T_C \qquad N_{\|} \to +\infty \tag{3}$$

where d is a dimension of a lattice, $\tilde{\sigma}$ is an unknown scaling function and $\tilde{\sigma}(x) \to$ constant as $x \to 0$ (Fisher *et al* 1973, Jasnow 1984). Here we use the hyperscaling relation $\mu = (d-1)\nu$ where μ and ν are the critical exponent for the interfacial free energy and for the correlation length respectively. This suggests $\sigma \sim N_\perp^{1-d}$ in the region where the correlation length diverges. At very low temperatures, where interfaces are assumed to be localized, we expect $\sigma \sim N_\perp^{0}$. Thus we assume for a whole temperature region

$$\sigma(T, N_\perp) \sim N_\perp^{a(T)} \qquad N_\perp \to +\infty \tag{4}$$

where a is an exponent of the size dependence of the interfacial free energy (Ono and Yamagata 1990, Yamagata and Ono 1990). If $a = 0$, we have an Ising-like long-range ordered phase, and if $a = -1$ in two dimensions we have a KT-like phase.

Here the dependence of $N_{\|}$ or $N_\perp/N_{\|}$ on σ might appear. As seen in subsection 3.1, there are no appreciable effects if $N_{\|}$ is set to be sufficiently large. Hereafter we have ignored the dependence of $N_{\|}$.

2.3. Helicity modulus

To investigate the phase transition between the KT-like phase and the disordered phase we consider a helicity modulus Υ defined by

$$\Delta f = \frac{1}{2}\left(\frac{\pi}{N_\perp}\right)^2 \Upsilon \tag{5}$$

where Δf is an excess free energy per spin (Fisher *et al* 1973). The helicity modulus was first introduced to study the phase transitions of isotropic spin systems, e.g. the Heisenberg model. The ordered phase of such systems has a continuous rotational symmetry in the ordered spin direction. The helicity modulus can describe the rigidity of the ordered phase against the twist. Though the ordered state in the 6-clock model has a discrete symmetry, Z_6, in the lowest temperature, we expect that this model behaves similar to the XY model in the KT-like phase and the disordered phase.

It can be seen simply that the helicity modulus is directly related to the excess energy ΔE, by

$$\frac{1}{2}\frac{\mathrm{d}(\beta\Upsilon)}{\mathrm{d}\beta} = \frac{1}{\pi^2}\frac{N_\perp}{N_{\|}}\Delta E \tag{6}$$

where $\beta = 1/T$ (Van Himbergen and Chakravarty 1981, Van Himbergen 1984). Thus we can get information for the helicity modulus through ΔE at a certain temperature without numerical integration.

Though the helicity modulus is defined in spin systems above, it may be applied to a Bose superfluid. In this case the helicity modulus is given by $\Upsilon = (\hbar/m)^2 \rho_s$ where ρ_s is a superfluid density (Fisher *et al* 1973). Since for the critical exponent η of the correlation function there is an equation $\eta = m^2 T/2\pi\hbar^2\rho_s$ where m is mass of a particle, we get a relation (Nelson and Kosterlitz 1977, Van Himbergen 1984)

$$\eta = \frac{1}{2\pi\beta\Upsilon}. \tag{7}$$

Hence we can obtain the critical exponent η through Υ without use of the finite-size scaling fitting.

3. Results

3.1. Interfacial free energy

Figure 1 shows the temperature variation of the excess energy per spin $\Delta\varepsilon$ for six lattice sizes in which $N_{\|}$ is fixed to be 50 and $N_{\perp}$ varies from 10 to 20. Error bars are calculated using the coarse-graining scheme (Landau 1976) i.e. standard deviations are obtained from their ten sub-averages. One can see that excess energies vanish at higher temperatures.

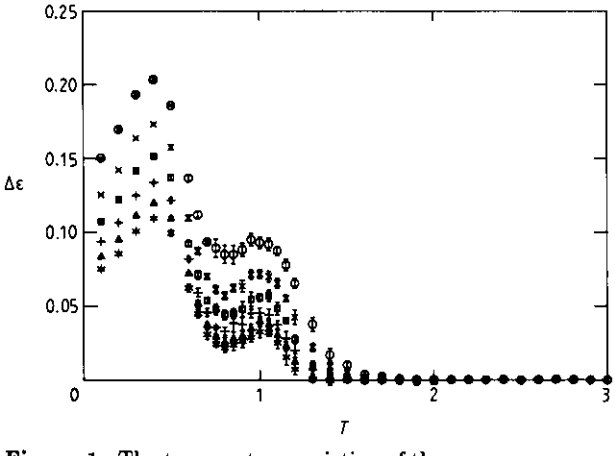

Figure 1. The temperature variation of the excess energy per spin between parallel and anti-parallel boundary conditions for the 6-clock model. Lattice sizes are as follows. $N_{\|} = 50$. $N_{\perp} = 10$, O; 12, ×; 14, □; 16, +; 18, Δ; 20, ∗.

Figures 2(a) and (b) show the $N_{\|}$ dependence of the excess energy per spin at several temperatures ($N_{\|} = 20,\ 50, 100,$ and $N_{\perp} = 20$). One sees that the $N_{\|}$ dependence is negligible within the statistical errors. Hereafter Monte Carlo simulations are confined to the fixed system of $N_{\|} = 50$.

The interfacial free energies are shown in figure 3(a) for six lattice sizes. We have $\sigma \simeq 3/2$ for all lattice sizes at $T = 0.1$. This indicates that the systems contain

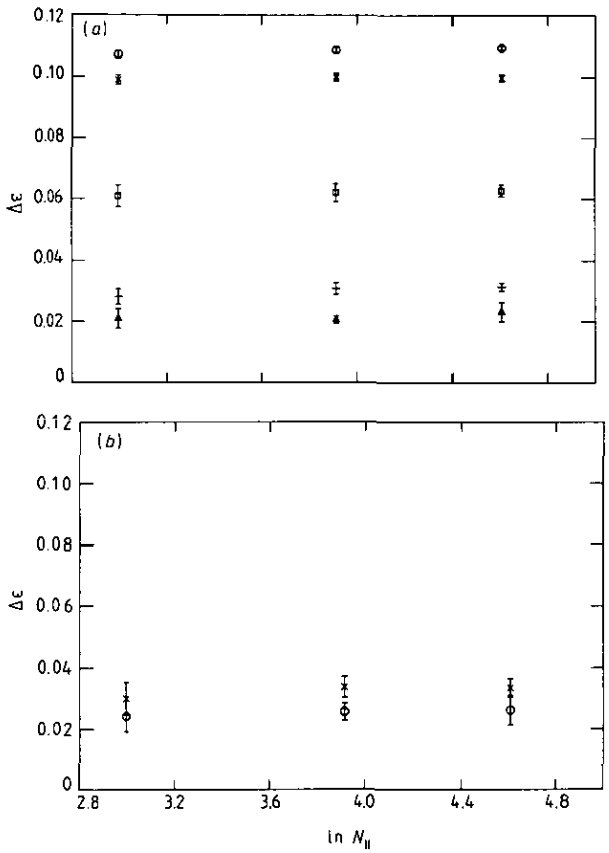

Figure 2. The $N_{\|}$ dependence of the excess energy per spin. Lattice sizes are as follows. $N_{\|} = 20, 50, 100$; $N_{\perp} = 20$. The figures attached indicate temperatures.

three flat interfaces at very low temperatures (see also figure 4(a)). The interfacial free energies decrease with increasing temperature and vanish at higher temperatures. One sees clearly that the interfacial free energies are dependent of the $N_{\perp}$ at intermediate temperatures. Figure 3(b) shows the log–log plots of σ against $N_{\perp}$ at various temperatures. The data for $\ln \sigma$ are found to be proportional to $\ln N_{\perp}$ as far as the temperature is lower than 1.0. The exponent a is determined by least-squares fitting in figure 3(b). The temperature variation of the exponent a is shown in figure 3(c). We can discriminate four phases as follows. (i) $T \leq 0.3$, $a \simeq 0$. This suggests that there are three flat and sharp interfaces in the systems and this phase is to be the Ising-like long-range ordered phase. (ii) $0.3 < T < 0.75$. The exponent a varies from 0 to -1 continuously. We do not know whether it is the intrinsic nature of this model or if the exponent changes from 0 to -1 discontinuously if $N_{\|} \to +\infty$. (iii) $0.75 \leq T \leq 0.9$, $a \simeq -1$. It suggests that this phase is a KT-like phase. (iv) $T > 0.9$, $a < -1$. The disordered phase.

It is clear that there exists a KT-like phase. The estimations of the transition temperatures are not so accurate, but will be comparable to those estimated by the MCRG or FC methods. Our values for lower and upper transition temperatures are $T_1 = 0.75$ and $T_2 = 0.90$ respectively. For comparison, Tobochnik (1982) obtained $T_1 = 0.6$ and $T_2 = 1.3$, Challa and Landau (1986) obtained $T_1 = 0.68 \pm 0.02$ and

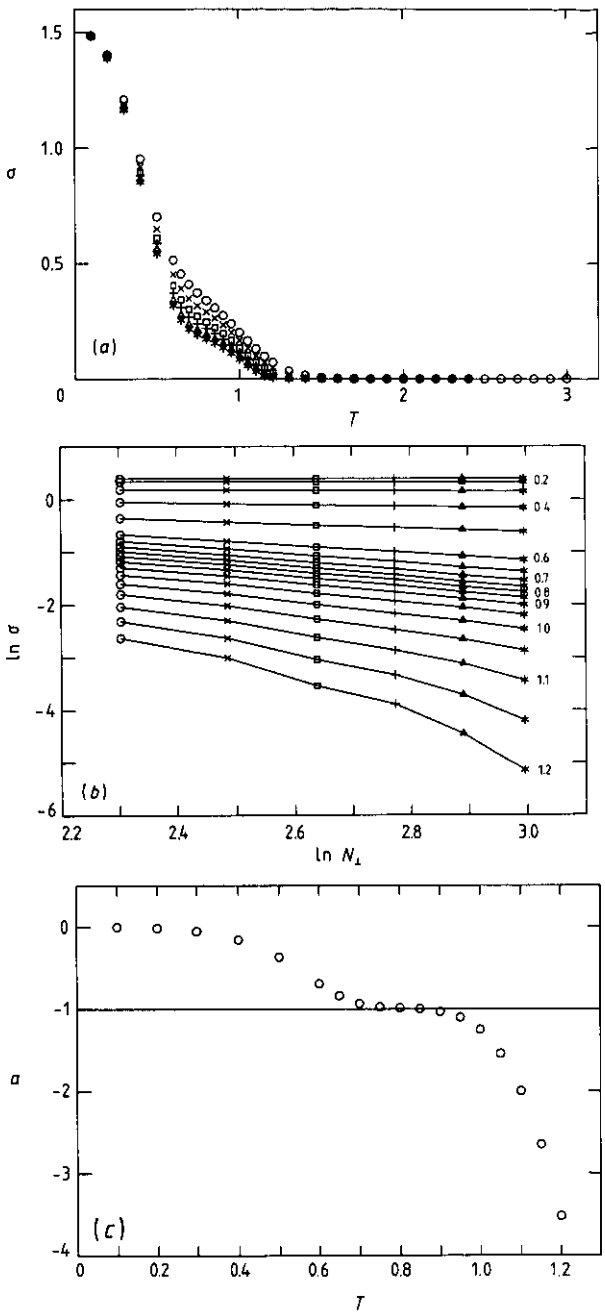

Figure 3. (*a*). The temperature variation of the interfacial free energy. Lattice sizes are as follows. $N_{\parallel} = 50$. $N_{\perp} = 10$, O; 12, ×; 14, □; 16, +; 18, Δ; 20, *. (*b*) The log–log plot of the interfacial free energy against $N_{\perp}$. The figures attached indicate temperatures. (*c*) The temperature variation of the exponent a for the $N_{\perp}$ dependence.

$T_2 = 0.92 \pm 0.01$. Our upper transition temperature T_2 should be compared with the transition temperature of the XY model, $T_C = 0.89, 0.898(2)$ obtained by other simulations (Tobochnik and Chester 1979, Fernández *et al* 1986, Gupta *et al* 1988).

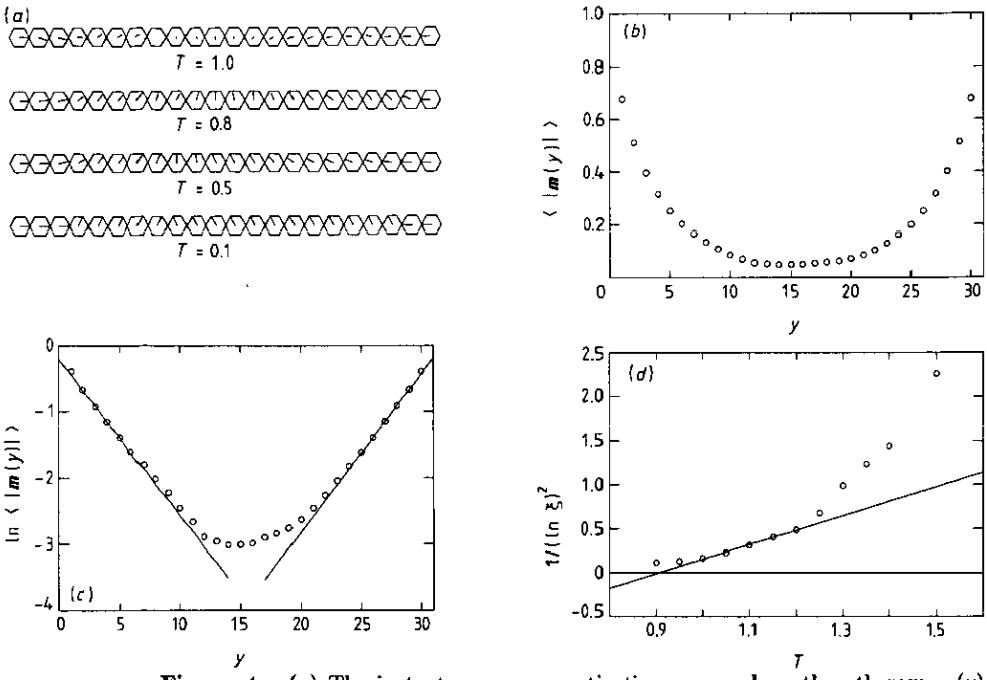

Figure 4. (*a*) The instantaneous magnetization averaged on the yth row $\boldsymbol{m}(y)$ for the system with the anti-parallel boundary condition is indicated with a line whose length is the amplitude $|\boldsymbol{m}(y)|$ in the yth hexagon from the left. ($N_{\|} \times N_{\perp} =$ 50 x 20, at 5 x10^3 MCS) (*b*) The magnetization $\langle|\boldsymbol{m}(y)|\rangle$ at $T = 1.2$ for the system ($N_{\|} \times N_{\perp} = 50 \times 30$) with the parallel boundary condition. The Monte Carlo averages are over 2 x 10^4 MCS after discarding 1 x 10^4 MCS. (*c*) The semi-log plot of $\langle|\boldsymbol{m}(y)|\rangle$ against y at $T = 1.2$. The full lines are drawn by the least-square fitting under the assumption that $\langle|\boldsymbol{m}(y)|\rangle \sim \exp(-y/\xi)$ and $\exp(-(N_{\perp}+1-y)/\xi)$ respectively. (*d*) The temperature just above T_2 variation of the correlation length, $1/(\ln\xi)^2$. The full line is drawn by least-squares fitting under the assumption that $\xi \sim \exp(bt^{-1/2})$ where b is a constant and $t = (T - T_2)/T_2$. From this figure we get $T_2 = 0.91$ and $b = 0.82$.

3.2. Magnetization profile

In addition to the interfacial free energy we estimate the magnetization profile. We divide the $N_{\|} \times N_{\perp}$ lattice into $N_{\perp}$ rows which consists of $N_{\|}$ spins. The magnetization for the yth row is defined as

$$\boldsymbol{m}(y) = \frac{1}{N_{\|}} \sum_{x=1}^{N_{\|}} (\cos\theta(x,y),\ \sin\theta(x,y))$$

where the sum is over $N_{\|}$ spins on the yth row. In figure 4(*a*) the instantaneous magnetization $\boldsymbol{m}(y)$ for the system with the anti-parallel boundary condition at the 5 x 10^3 MCS is indicated with a line whose length is an amplitude $|\boldsymbol{m}(y)|$ in a yth hexagon from the left ($N_{\|} \times N_{\perp} = 50 \times 20$). As described in subsection 2.1, since all $N_{\|}$ spins on boundaries for the unfavourable system are fixed to be anti-parallel as $\boldsymbol{m}(0) = (1,0)$ and $\boldsymbol{m}(N_{\perp}+1) = (-1,0)$. According to the results in figure 3(*c*) we may clarify the characteristic spatial variations of the instantaneous magnetization into four temperature regions. (i) The ordered phase ($T = 0.1$): the directions of $\boldsymbol{m}(y)$ are parallel and the amplitudes of $\boldsymbol{m}(y)$ are saturated values in each domain.

Sharp interfaces appear between the different domains. Their locations are between $y = 2$ and $y = 3$, $y = 7$ and $y = 8$, and $y = 19$ and $y = 20$. (ii) The transitive phase ($T = 0.5$): the amplitudes $|\boldsymbol{m}(y)|$ are less than 1 except near boundaries, and interfaces are not sharp and diffuse. The direction of $\boldsymbol{m}(y)$ apparently rotates, but not in a single harmonic way. (iii) The KT-like phase ($T = 0.8$) : the direction of $\boldsymbol{m}(y)$ rotates smoothly as

$$\boldsymbol{m}(y) \sim |\boldsymbol{m}(y)|\left(\cos\left(\frac{\pi}{N_\perp}y\right), \sin\left(\frac{\pi}{N_\perp}y\right)\right).$$

The amplitudes of $\boldsymbol{m}(y)$ become shorter than those at $T = 0.5$ in (ii). (iv) The disordered phase ($T = 1.0$): the amplitude of $\boldsymbol{m}(y)$ vanishes $|\boldsymbol{m}(y)| \simeq 0$ except around the boundaries.

We propose a method to get a correlation length as follows. In figure 4(b) we show the magnetization $\langle|\vec{m}(y)|\rangle$ ($\langle\cdots\rangle$ denotes Monte Carlo averages.) at $T = 1.2$ for the system ($N_\parallel \times N_\perp = 50 \times 30$) with the parallel boundary condition. From figure 4(b) one sees the magnetization $\langle|\boldsymbol{m}(y)|\rangle$ decays exponentially as the distance y or $N_\perp + 1 - y$ from the boundary is increasing. Its decay is assumed to obey the correlation length ξ as $\langle|\boldsymbol{m}(y)|\rangle \sim \exp(-y/\xi)$ or $\exp(-(N_\perp + 1 - y)/\xi)$. Figure 4($c$) shows the semi-log plots of $\langle|\boldsymbol{m}(y)|\rangle$ against y at $T = 1.2$. Near the boundary one sees $\ln\langle|\boldsymbol{m}(y)|\rangle$ is proportional to y or $N_\perp + 1 - y$ except for neighbours at the boundary. Therefore we get the correlation length at $T = 1.2$ from the slope in figure 4(c). If the 6-clock model has a KT-like phase, its correlation length behaves as $\xi \sim \exp(bt^{-1/2})$ just above T_2, where b is a constant and $t = (T - T_2)/T_2$. Figure 4(d) shows the temperature variation of $1/(\ln\xi)^2$. Just above T_2 ($= 0.9$) one sees that $1/(\ln\xi)^2$ is proportional to T. Thus we get the upper transition temperature T_2 to be 0.91 and the constant b to be 0.82 from figure 4(d). The value for T_2 agrees with the result estimated from the exponent a within about 1%. The value of the constant b does not agree with the theoretical result 1.5 for the XY model (Kosterlitz 1974) and $b = 1.54 \pm 0.01$ obtained by Challa and Landau (1986).

3.3. Helicity modulus

In figure 5(a) the data for $(1/\pi^2)(N_\perp/N_\parallel)\Delta E$ of the right-hand side in (6), are plotted against temperature. The height of the peak increases and its position decreases toward the upper transition temperature T_2 with increasing lattice size. The latter behaviours are different from those of the XY model. Van Himbergen (1984) found for the XY model that the positions of the peaks were independent of lattice sizes and were located at $T = 0.970 \pm 0.005$. For the 6-clock model we reported earlier that the peaks were located at $T = 1.0$ irrespective of lattice sizes (Yamagata and Ono 1990). It was because the sizes $N_\perp$ were too small ($N_\perp = 8,\ 12,\ 16, 20,$ and $N_\parallel = 20$). Figure 5(b) shows that the height of the peak increases in proportion to $\ln N_\perp$. This indicates that in the thermodynamic limit the helicity modulus has a finite jump at T_2. This jump corresponds to the universal jump of the superfluid density in helium films (Nelson and Kosterlitz 1977, Bishop and Reppy 1978). These behaviours are same as those of the XY model. Thus the phase transition between the intermediate phase and the disordered phase can be concluded to be of the KT type. This is consistent with the results in figure 4(d) or the relation $\xi \sim \exp(bt^{-1/2})$.

Figure 6(a) shows the temperature variation of the helicity modulus for the six sizes of lattices. Here we used the relation $\Upsilon = 2N_\perp\sigma/\pi^2$ (see equation (5)). It is clear

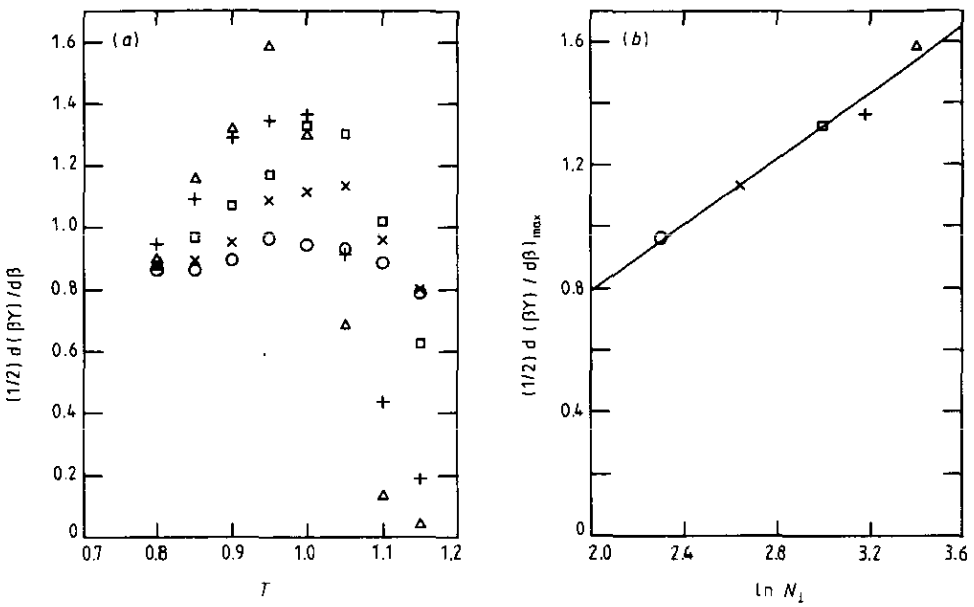

Figure 5. (*a*) The temperature variation of $(1/\pi^2)(N_\perp/N_\parallel)\Delta E$. (*b*) The $N_\perp$ dependence of the peak height. Lattice sizes are as follows. $N_\parallel = 50$. $N_\perp = 10$, ○; 14, ×; 20, □; 24, +; 30, △.

that the helicity modulus has no size dependence in the region of $0.75 \leq T \leq 0.90$ because σ is found to be proportional to $N_\perp^{-1}$ in this region. Figure 6(*b*) shows the temperature variation of the critical exponent η for the correlation function using equation (7). We see that the critical exponent η varies from 0.15 at T_1 to 0.26 at T_2. Analysis of the Villain model which has the same symmetry with the 6-clock model predicts that η varies from 1/9 to 1/4 in the intermediate phase (José *et al* 1977, Elitzur *et al* 1979). Other results by different methods are shown in addition to our result. Our result is slightly higher, within 3%, than the theoretical value of T_2.

4. Summary

We have concluded that there exists a KT-like phase between the Ising-like long-range ordered phase and the disordered phase, and that lower and upper transition temperatures are given by $T_1 = 0.75$ and $T_2 = 0.90$, respectively, from the exponent of the size dependence of the interfacial free energy. We have proposed the method to get the correlation length ξ from the distance dependency of the magnetization profile. Under the assumption $\xi \sim \exp(bt^{-1/2})$ we have $T_2 = 0.91$ and $b = 0.82$. The transition at T_2 has been concluded to be of KT-type since the temperature derivative of the helicity modulus may diverge in the thermodynamic limit. We have estimated the critical exponent η in the intermediate temperatures, which varies from 0.15 at T_1 to 0.26 at T_2.

Finally one should note that the above phenomena are similar to those of the AFP model which has weak next-nearest-neighbour ferromagnetic interactions (Ono and Yamagata 1990). This will be related to the fact that the model has six ground states (Ono 1984). The details are left for a forthcoming paper.

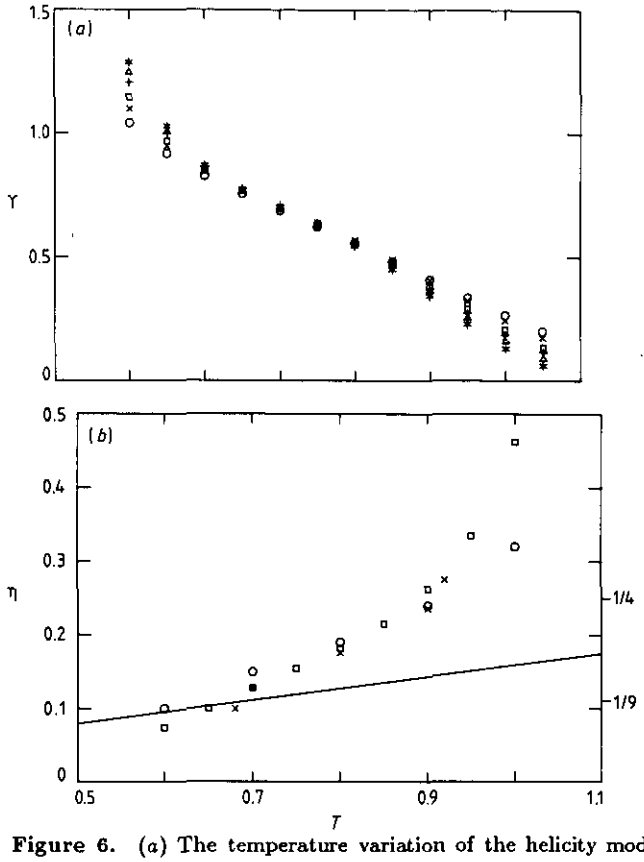

Figure 6. (*a*) The temperature variation of the helicity modulus. Lattice sizes are as follows. $N_{\|} = 50$. $N_{\perp} = 10$, ○; 12, ×; 14, □; 16, +; 18, △; 20, *. (*b*) The temperature variation of the exponent η. The square indicates the result of this work ($N_{\|} \times N_{\perp} = 50 \times 20$). The circle and the cross indicate the results by Tobochnik (1982) and Challa and Landau (1986) respectively. The full line is the spin wave result ($\eta = T/2\pi$). The numbers on right side in this figure are values from analysis on the Villain model.

Acknowledgments

We wish to thank Y Tamura for use of the computer HITAC M-682H of the Institute of Statistical Mathematics. Monte Carlo simulations have partially been carried out on the computer HITAC S-820/80 of the Institute for Molecular Science.

References

Baxter R J 1982 *Proc. R. Soc.* A **383** 43
Binder K (ed) 1979 *Monte Carlo Methods in Statistical Physics* (Berlin: Springer)
—— 1984 *Applications of the Monte Carlo Method in Statistical Physics* (Berlin: Springer)
Bishop D J and Reppy J D 1978 *Phys. Rev. Lett.* **40** 1727
Cardy J L 1981 *Phys. Rev.* B **24** 5128
Challa M S S and Landau D P 1986 *Phys. Rev.* B **33** 437
Chui S T and Weeks J D 1976 *Phys. Rev.* B **14** 4978
Elitzur S, Pearson R B and Shigemitsu J 1979 *Phys. Rev.* D **19** 3698
Fernández J F, Ferreira M F and Stankiewicz J 1986 *Phys. Rev.* B **34** 292

Fisher M E, Barber M N and Jasnow D 1973 *Phys. Rev.* A **8** 1111
Grest G S and Banavar J R 1981 *Phys. Rev. Lett.* **46** 1458
Gupta R, DeLapp J, Batrouni G G, Fox G C, Baillie C F and Apostolakis J 1988 *Phys. Rev. Lett.* **61** 1996
Ito N and Kanada Y 1988 *Supercomputer* **5** 31
Jasnow D 1984 *Rep. Prog. Phys.* **47** 1059
Jayaprakash C and Tobochnik J 1982 *Phys. Rev.* B **25** 4890
José J V, Kadanoff L P, Kirkpatrick S and Nelson D R 1977 *Phys. Rev.* B **16** 1217
Kosterlitz J M 1974 *J. Phys. C: Solid State Phys.* **7** 1046
Kosterlitz J M and Thouless D J 1973 *J. Phys. C: Solid State Phys.* **6** 1181
Landau D P 1976 *Phys. Rev.* B **13** 2997
Mermin N D and Wagner H 1966 *Phys. Rev. Lett.* **17** 1133
Metropolis N, Rosenbluth A W, Rosenbluth M N, Teller A H and Teller E 1953 *J. Chem. Phys.* **21** 1087
Nelson D R and Kosterlitz J M 1977 *Phys. Rev. Lett.* **39** 1201
Ono I 1984 *J. Phys. Soc. Japan* **53** 4102
Ono I and Yamagata A 1990 *J. Magn. Magn. Mat.* to appear
Tobochnik J 1982 *Phys. Rev.* B **26** 6201; 1983 *Phys. Rev.* B **27** 6972 (erratum)
Tobochnik J and Chester G V 1979 *Phys. Rev.* B **20** 3761
Ueno Y, Sun G and Ono I 1989 *J. Phys. Soc. Japan* **58** 1162
Van Himbergen J E 1984 *J. Phys. C: Solid State Phys.* **17** 5039
Van Himbergen J E and Chakravarty S 1981 *Phys. Rev.* B **23** 359
Villain J 1975 *J. Physique* **36** 581
Wang J S, Swendsen R H and Kotecký R 1989 *preprint*
Wu F Y 1982 *Rev. Mod. Phys.* **54** 235
—— 1984 *J. Appl. Phys.* **55** 2421
Yamagata A and Ono I 1990 *J. Magn. Magn. Mat.* to appear